

Microstructural features and final mechanical properties of the iron-modified Al-20Si-3Cu-1Mg alloy product processed from atomized powder

J. ZHOU, J. DUSZCZYK, B. M. KOREVAAR

Laboratory for Materials Science, Delft University of Technology, Rotterdamseweg 137, 2628 AL Delft, The Netherlands

The potential piston alloy Al-20Si-5Fe-3Cu-1Mg has been experimentally extruded from rapidly solidified powder, and subsequently heat treated. The effects of adding iron to the alloy on the microstructural evolution during the solution and ageing treatment subsequent to extrusion have been examined. The study shows that iron-bearing intermetallic particles modify the recrystallization behaviour of the present alloy during solution treatment at 470 °C in a complex way, through blocking the migration of recrystallized grain boundaries from particle-depleted areas, and pinning subgrain boundaries in particle-rich areas, thus leading to a partially recrystallized duplex structure in the final product. The observed two-fold role of the intermetallic particles is a consequence of their inhomogeneity in distribution, which in turn results from the processing history of the powdered alloy. It is also observed that, in the presence of the intermetallic particles, the excessive coarsening of the silicon particles dispersed in the α -Al matrix (as occurs to the base alloy during the heat treatment) is lessened. The retained subgrain boundaries provide heterogeneous nucleation sites for precipitation occurring during ageing. Most of the precipitates are characterized by being associated with iron, and the precipitating behaviour of copper and magnesium in the present alloy with the iron addition is accordingly altered. The resultant tensile properties of the alloy at room and elevated temperatures have been assessed, with reference to those of the base Al-Si-Cu-Mg alloy. The results indicate that the present alloy with the iron addition has a fairly high hot strength up to a temperature of 300 °C, which offers an important improvement ensuring its reliable application in automotive engines.

1. Introduction

Hypereutectic Al-Si alloys are known to be suitable for use as piston materials. The key to the easy processing and successful application of the alloys lies in producing and maintaining a microstructure with very fine silicon particles throughout a fabrication cycle. In order to achieve this, various modifications in alloying composition have been made. Addition of sodium, strontium or phosphorus has been found to be effective in suppressing the formation of coarse primary silicon particles in the as-cast microstructure of the alloys [1-3]. Also, new techniques such as rheocasting [5, 6] and rapid solidification have been developed. Among these techniques, rapid solidification appears to give the most marked benefits, and thus has been an area of immense interest in recent years. Numerous processes, from splat quenching, rotating water atomization, gas atomization and spray deposition to melt spinning, have emerged [7-11]. Moreover, further attempts to reduce the silicon particle size have been made by combining the two approaches, that is, adding a refining element like

strontium, chromium or cobalt and at the same time applying rapid solidification [12, 13]. Application of the above processes can offer a satisfactory solution to the Al-Si alloy production, although the extent depends critically on the particular type of processes employed and the processing conditions. Therefore, in general, the primary problem of coarsened silicon particles initially encountered in the hypereutectic Al-Si alloy fabrication has been solved. Lately, attention has been shifted to further improvement in the service properties of rapidly solidified Al-Si alloys, hot strength in particular, because the alloys are required to serve at high temperatures, for example in automotive engines. In order to ensure their reliable application in such a service condition, a modification in alloying composition, specifically aimed at enhancing their thermal stability, has been introduced.

Iron is often added to aluminium alloys to enhance their heat resistance. Added in a certain percentage to Al-Si alloys, it forms a volume fraction of thermally stable intermetallic phases, and as a result gives a considerable improvement in the high-temperature

performance of these materials. This improvement has recently been reported in several communications [14–16]. Apparently, a modification in the chemical composition of the alloys leads to an alteration in the structure and resultant properties. However, no detailed work regarding the effects of iron addition on the characteristics of the processing, microstructure and mechanical properties of the rapidly solidified Al–Si alloys at each stage of a fabrication cycle has been reported, despite its obvious importance. In a previous paper [17], we have described the microstructural development, from the atomized powder particles to the consolidated extrudates of the Al–20Si–3Cu–1Mg alloy with 5% iron addition. The current work focuses on the subsequent part of the integral processing cycle of the alloy: the effects of iron addition on the microstructural evolution during solution and ageing treatment following consolidation, and its impact on the mechanical properties of the final product at room and elevated temperatures.

2. Experimental procedure

The alloy, with a nominal composition of 20 wt % Si, 5 wt % Fe, 3 wt % Cu, 1 wt % Mg and balance aluminium, was supplied by Showa Denko K. K., Japan, in the form of air-atomized powder. The characteristics of the as-received powder particles and the details of sequential processing including precompaction, degassing and extrusion have been described at length in a companion paper [17]. Here only the extrusion conditions that are directly related to the subsequent heat treatment response of the alloy are given. The consolidation of the powder by extrusion was performed at a temperature of 375 °C, a reduction ratio of 20:1, and a ram speed of 5 mm s⁻¹.

As this alloy contains the precipitation strengthening elements copper and magnesium, a solution and ageing treatment is generally regarded as normal practice in order to develop the full strength of the final product. In the present work, a commercially used scheme of heat treatment for the alloy series, T6 temper, was applied: this involved solution treating at 470 °C for 1.5 h followed by water quenching, natural ageing for 4 days, and artificial ageing at 120 °C for 24 h.

The microstructure of the iron-modified Al–Si–Cu–Mg alloy before and after the heat treatment was observed and compared with that of the base alloy. Specimens for optical and electron microscopy were prepared on transverse sections of the extruded and subsequently T6-tempered product. The optical specimens were etched with a dilute Keller & Wilcox's reagent, and observation was made by means of a Neophot-2 (Carl Zeiss, Jena) microscope. The foil specimens for transmission electron microscopy were finally thinned using an ion mill at a current of 0.5 mA and a gun inclination of 20°. A Philips 400 T electron microscope operating at 120 kV was used for observation, and the attached X-ray energy dispersive spectrometry (EDS; Tracor system) was used to aid phase identification.

Tensile tests on the alloy at room and elevated

temperatures, in both the as-extruded and as-heat treated states, were carried out at an initial strain rate of $5.6 \times 10^{-3} \text{ s}^{-1}$. A Tira test 2300 machine with a split furnace was used. Cylindrical specimens were machined to be coaxial with the extrusion direction and to have a gauge length to diameter ratio of 5. They were heated at their testing temperatures for 100 h before testing so as to simulate the service conditions of the alloy. The fracture surfaces of the specimens were observed using a Jeol JXA-50A scanning electron microscope (SEM) at 15 kV.

3. Results and discussion

3.1. The effect of iron addition on recrystallization behaviour

Fig. 1a presents a typical micrograph of the extruded alloy prior to the heat treatment, which depicts predominantly a deformed microstructure. It features numerous microcells associated with second-phase particles, even though some preliminary recrystallization at some preferential sites (for example, nearby silicon particles) can be observed, as shown in Fig. 1b. The general as-extruded microstructure of the present alloy is not significantly different from that of the base Al–Si–Cu–Mg alloy processed under the same conditions [18].

As the alloy has undergone a large deformation during extrusion which has introduced a high stored-strain energy, the alloy has a strong driving force to be statically recovered and recrystallized afterwards, depending on temperature and time. Soaking at 470 °C for 1.5 h during the solution treatment in the T6 temper, as applied to the extruded alloy, principally permits extensive restoration, unless there is a large resistance. The presence of a high volume fraction of silicon particles in the present alloy, with sizes ranging from 0.5 to 3 µm, generally promotes the nucleation of recrystallization [19, 20]. Moreover, during solution treating the dissolution of copper- and magnesium-bearing precipitates in the alloy, which have been formed before the heat treatment, further facilitates the completion of restoration. This is because the precipitates which are associated with subgrain boundaries or cell walls can easily dissolve in view of a relatively higher energy there. As a result, the barriers to the motion of subgrain and grain boundaries (arrows, Fig. 1b) are lifted. Therefore, according to the kinetic theory of recrystallization which has been developed primarily for conventional aluminium alloys, the T6 temper heat treatment seems to enable most of the worked microstructure to be recrystallized, as observed in the Al–Si–Cu–Mg base alloy (Fig. 2). However, the observation of the present iron-modified alloy after the full treatment reveals a different microstructure that consists of a mixture of deformed, unrecrystallized and recrystallized grains, as shown in Fig. 3. The former is characterized by clustered second-phase particles, while the latter lacks interior particles. In comparison with Fig. 2, which is obtained under the same processing conditions, the difference in the resultant recrystallization level obviously arises from the addition of iron which forms a

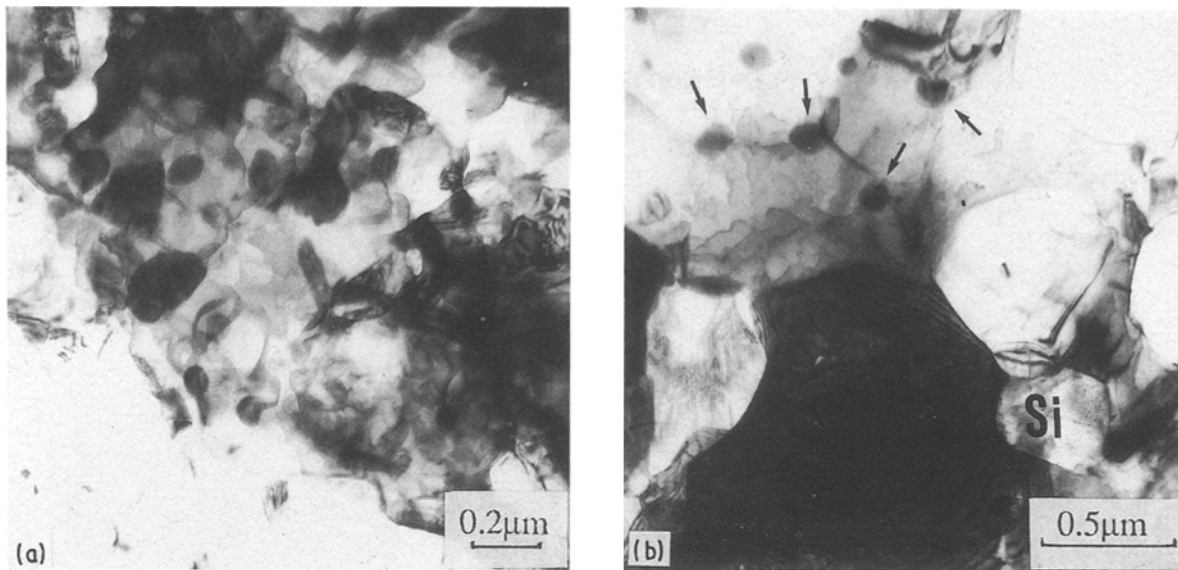


Figure 1 Electron micrographs of Al-Si-Fe-Cu-Mg alloy in the as-extruded state, showing (a) numerous microcells associated with second-phase particles, and (b) occurrence of preliminary recrystallization in the vicinity of large particles.

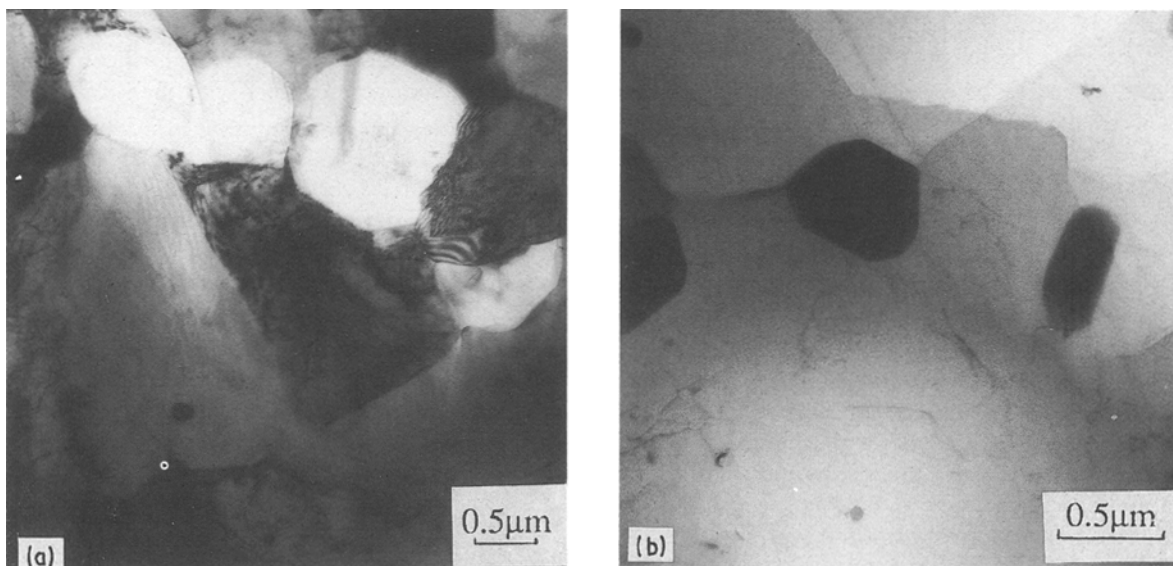


Figure 2 Electron micrographs of Al-Si-Cu-Mg base alloy in the as-T6 tempered state, showing (a) recrystallization stimulated by silicon particles, and (b) recrystallized grains depleted of interior dislocations.

high volume fraction of indissoluble intermetallic particles. It should be noted that these particles are not homogeneously distributed, but in clusters, as can clearly be seen from Fig. 3. This kind of inhomogeneous distribution on a microscale is a common feature of the complex microstructure of practical, technologically important alloys. Although only a few investigations on restoration processes have been devoted to such non-ideal, complicated aluminium alloys, it has been recognized that the inhomogeneity in fine-particle distribution can exert a considerable influence on the mechanisms of recrystallization [21]. For the present alloy, the formation of the inhomogeneity in the intermetallic particle distribution is obviously related to its processing history. During atomization, intermetallic phases are formed in a size range strongly

related to the powder particle size with a wide variation [17]. More importantly, during extrusion the intermetallics, initially present in needles with differing sizes in the atomized powder particles, are broken up and redistributed by metal flow, thus giving rise to a marked variation in interspacing between the fragmented intermetallics. The influence of these inhomogeneously distributed intermetallic particles on the recrystallization behaviour during the heat treatment is of considerable interest. The effect of the copper- and magnesium-bearing precipitates on the evolution of the matrix microstructure during solution treating is considered to be of relatively minor importance, because the recrystallization is assumed to take place after their dissolution during solution treating but before their reprecipitation as a response to ageing.

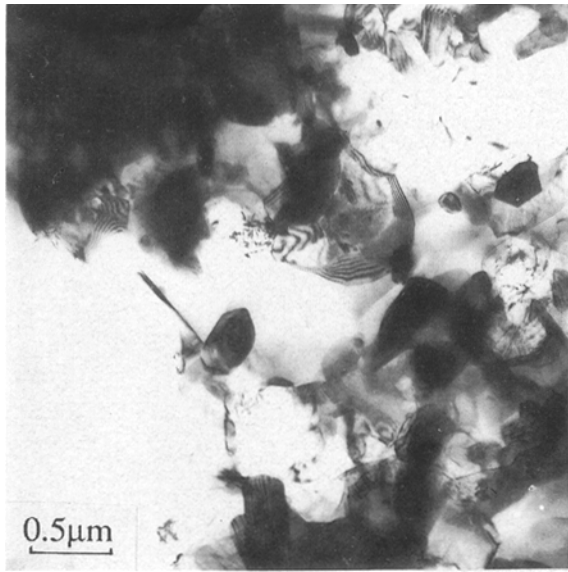


Figure 3 Electron micrograph of Al-Si-Fe-Cu-Mg alloy in the as-T6 tempered state, showing a partially recrystallized structure.

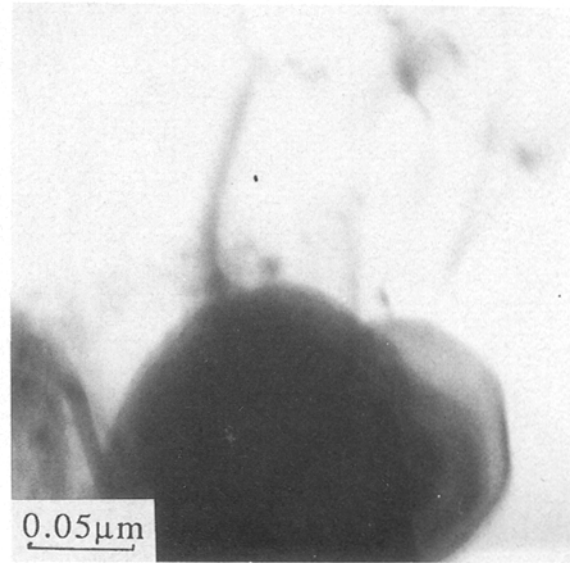


Figure 4 Recrystallized area in Al-Si-Fe-Cu-Mg alloy after T6 temper, illustrating traces of original subgrain boundaries linked with a second-phase particle.

It can be seen from Fig. 3 that in the particle-depleted areas, the original deformed microstructure is recrystallized to be essentially free of dislocations. However, the growth of recrystallized grains is hindered by clusters of second-phase particles. In some recrystallized areas, faint traces of original subgrain boundaries which are usually attached to the fine particles are still observable at very high magnification in the electron microscope (Fig. 4). It is confirmed that most of the recrystallized grains are indeed originated in the vicinity of relatively large particles, near either silicon particles or intermetallic particles, as shown in Fig. 5. This implies that in these areas the major recrystallization mechanism is nucleation of new grains, rather than subgrain rotation and subgrain boundary migration. The electron micrograph shows that the recrystallized grains are moving into the surrounding deformed matrix. X-ray EDS

indicates that the intermetallic particles are aluminium based, containing iron and silicon. Electron diffraction analysis together with the phase constitution analysis of Al-Fe-Si alloys [22], suggests that the particles are likely to be β -AlFeSi equilibrium phase [23]. No appreciable coarsening of intermetallic particles during solution treating can be observed, confirming their high thermal stability.

Interestingly, there is evidence that some recrystallized grain fronts have passed round scattered, single particles, and left them behind with dislocation loops, as illustrated in Fig. 6a. The detachment of the recrystallized grain boundaries from the particles indicates that in this case the driving force for recrystallization overcomes the resistance exerted by the particles:

$$F_R > 3f\gamma/2r$$

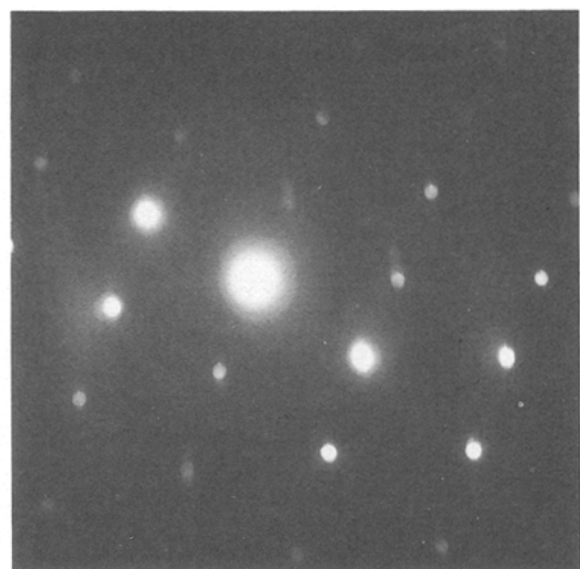
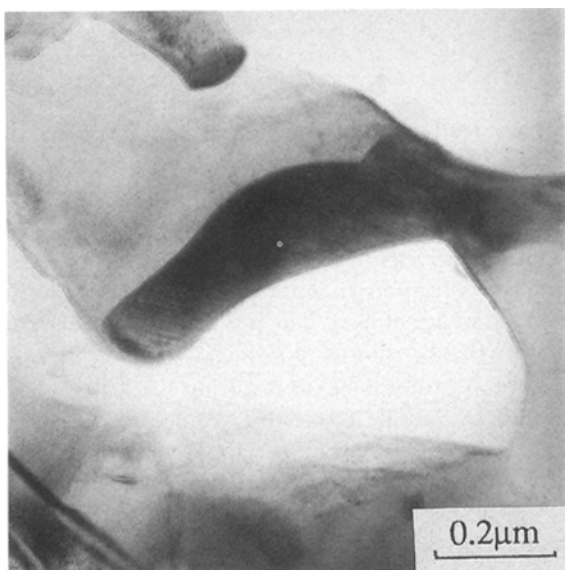


Figure 5 An intermetallic particle and its diffraction pattern, with multiple recrystallization nucleation occurring around it.

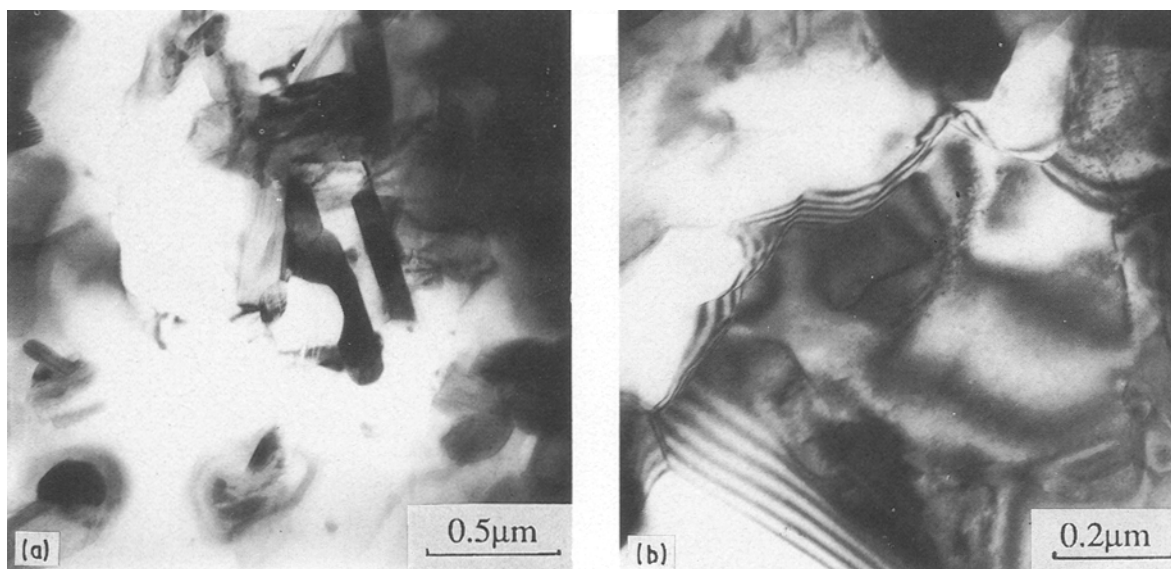


Figure 6 Electron micrographs showing (a) recrystallized grains growing into deformed matrix and passing round the single particles, and (b) growth of recrystallized grains blocked by clusters of particles.

where F_R is the driving force for recrystallization, f and r are the volume fraction and radius of second-phase particles, respectively, and γ is boundary energy per unit area. The present study confirms that the interspacing between dispersed particles is a decisive factor for the growth kinetics of recrystallized grains. It means that passing round closely spaced particles is much more difficult and thereby an increased thermal energy is required. Fig. 6b shows that only the particles in a cluster can prevent the migration of recrystallized grain front composed of grouped dislocations. This phenomenon can easily be observed by manipulating the tilt controls of the microscope. Because the intermetallic phases in the present alloy are very stable, heating to a higher temperature may still not allow extensive recrystallization to occur. Hence the inhibited grain growth in the deformed matrix can be one of the inherent features of the worked alloy with a high volume fraction of indissoluble particles. It is also found that in a few regions no blocking particles around recrystallization nuclei are observable, but their growth into the deformed matrix is stopped without apparent reason. The implication is that a state of balance between growth and resistance is attained there. This phenomenon has also been noticed in other aluminium alloys [24, 25], and may be attributable to the reduced driving force of some recrystallization nuclei and differing growth circumstances. As a result of the recrystallization characteristics exhibited by the present alloy, many recrystallized grains are found to be irregular in shape, some being island shaped and surrounded by deformed matrix, and their sizes varying greatly between 0.2 and 1.0 μm .

The unrecrystallized areas are usually rich in second-phase particles, which pin either dislocation tangles of high density or distinct subgrain boundaries, as indicated by the arrows in Fig. 7. During heating and soaking, the original microcells merge to a certain extent into well-defined subgrains, and the

subgrain boundaries become thinned. The typical deformed structure in these areas, however, is almost unaltered, as compared to the microstructure in the as-extruded state [17]. Evidently, in the areas with fine, closely spaced particles the nucleation of new recrystallization nuclei is effectively suppressed. Moreover, subgrain coalescence, as an alternative mechanism of recrystallization, cannot be operative because the subgrain boundaries are strongly pinned by the intermetallic particles, especially at triple junctions. Consequently the exposure of the present alloy to 470 °C for 1.5 h in the T6 temper cannot bring about complete recrystallization, and thus the worked structure in the particle-rich areas is retained. The present study on this highly alloyed aluminium supports a previous finding that the influence of fine particles on the static recrystallization rate can be more than three orders of magnitude [26].

From the above, it is clear that the clusters of iron-bearing intermetallics in the present alloy simultaneously play a dual role, that is, blocking the growth of recrystallized grains from particle-depleted areas as discussed earlier, and pinning the migration of subgrain boundaries in particle-rich areas. This two-fold role is apparently assigned by the inhomogeneous distribution of the particles, as a consequence of the processing characteristics of the alloy prepared from atomized powder. This kind of complex influence of the second-phase particles, although often encountered in commercial alloys [27], is difficult to observe in the simple aluminium alloys usually used in recrystallization studies. The current work suggests that generalizing the influence of second-phase particles on recrystallization mechanisms is difficult, particularly for the rapidly solidified, powdered alloys, because of their inherent microstructural features and special processing procedures. Therefore it is important to understand the recrystallization features of rapidly solidified and subsequently worked aluminium alloys, although difficulties may be encountered in revealing

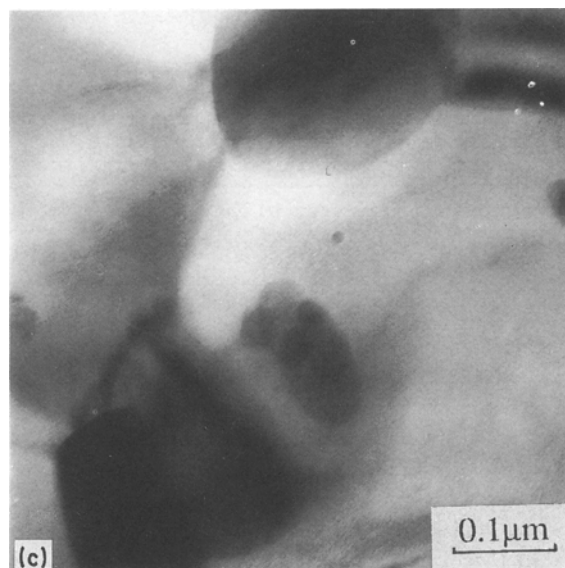
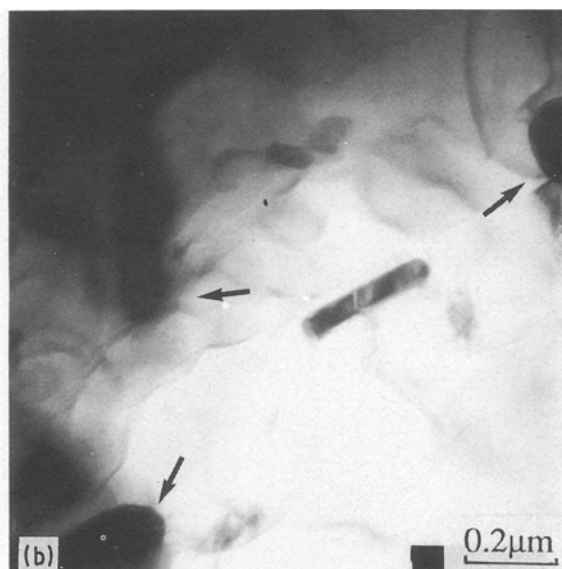
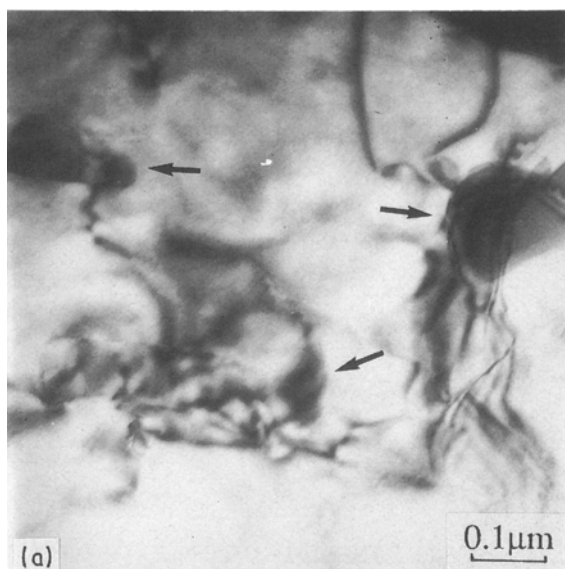


Figure 7 Electron micrographs of the T6-tempered Al-Si-Fe-Cu-Mg alloy showing (a) retained dislocation tangles, (b) subgrains, and (c) interaction between second phase particles and subgrain boundaries.

microstructure, identifying phases, and controlling second-phase particle size and distribution.

3.2. The effect of iron addition on silicon particle coarsening

As mentioned above, maintaining fine silicon particles throughout a fabrication cycle is a crucial factor for the processing and application of the alloy. It has been shown that in the Al-Si-Cu-Mg base alloy, silicon particle size is fairly sensitive to extrusion temperature. Particularly above 400 °C, the coarsening of silicon particles becomes very obvious [18]. Furthermore, the silicon particles dispersed in the α -Al matrix of the base alloy have a strong propensity to coarsening when exposed to high temperatures during solution treating, which may in turn promote the recrystallization of the matrix [20].

In the present alloy with iron addition, however, silicon particle size appears much less sensitive to extrusion temperature than that of the base alloy. Also, after the T6 temper there is little discernible increase in the silicon particle size, as shown in Fig. 8.

This feature offers one of the major advantages of the present alloy. Under identical processing conditions, the addition of iron is the only possible factor that can account for this observation. It is probable that the activity of silicon is reduced due to the interaction between the silicon particles and Al-Fe-Si intermetallics or even the incorporation of iron in the silicon particles. Another explanation may be that the coarsening of silicon particles proceeds through the diffusion of silicon atoms over a long distance from one particle to another, occurring preferentially along grain and subgrain boundaries because the activation energy for pipe diffusion is lower than for volume diffusion. The addition of 5% iron creates a high volume fraction of dispersed intermetallic phases which are broken up during extrusion and redistributed on a fine scale at grain and subgrain boundaries, as well as within grains. These may act effectively as sinks for vacancies and obstacles to the diffusion of silicon atoms over a long distance, particularly along the grain and subgrain boundaries with which the intermetallic particles interact. As a result, the growth of silicon particles becomes difficult and their coarsening rate is relatively slowed down. Such an explanation has also been applied to a similar phenomenon occurring in a mechanically alloyed Al-Fe-Ce alloy with introduced oxides and carbides which make the coarsening of dispersoids difficult [28]. Therefore, in addition to providing dispersion strengthening and modifying matrix microstructural development, the additive iron may also play an important role in lessening the coarsening of silicon particles in the Al-Si alloy.

3.3. Precipitation characteristics

For a given alloy the precipitation process is mainly controlled by the degree of supersaturation, ageing

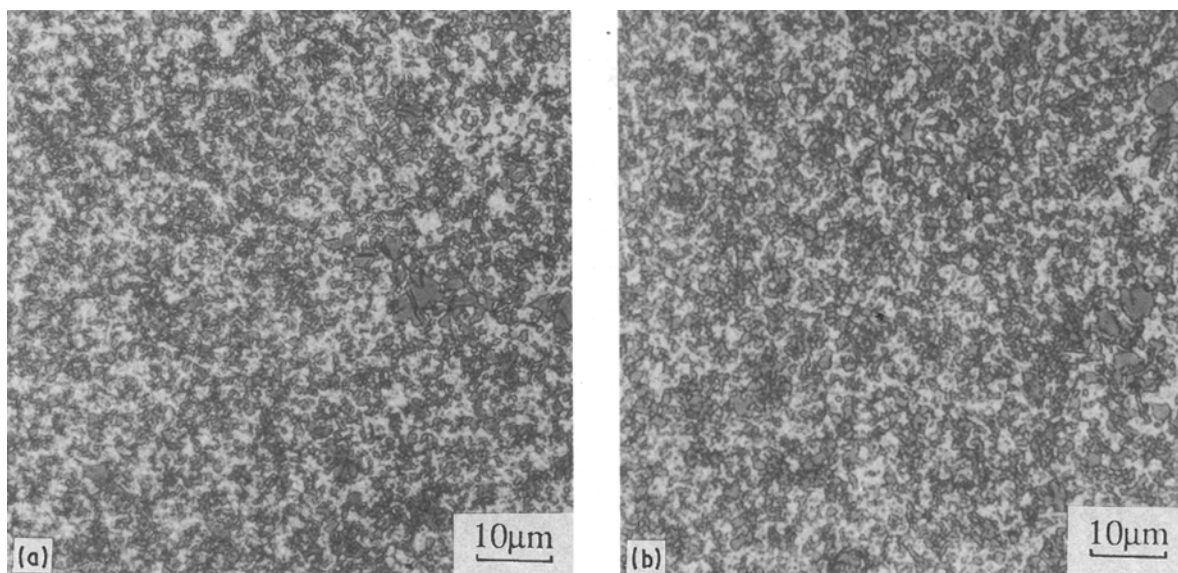


Figure 8 Optical micrographs of Al-Si-Fe-Cu-Mg alloy comparing the silicon particle size (a) before and (b) after T6 temper.

temperature and duration, and the availability of vacancies and heterogeneous nucleation sites [29]. For the present alloy which is rapidly solidified during powder production, precipitation tends to happen during hot extrusion and subsequent air cooling, because deformation accompanied by dislocation generation can effectively facilitate the heterogeneous nucleation of precipitates [30]. These precipitates are found to be present in the as-extruded material (see Fig. 1), and most of them are detected with X-ray energy dispersive analysis to be Al-Si-Cu-Fe phase. Some of these precipitates are believed to dissolve in the matrix during solution treating and then to re-precipitate out as a response of ageing, because after the T6 temper the size of the precipitates has decreased and the density increased. It is also observed that most of the precipitates lie at the subgrain boundaries, as shown in Fig. 9. This indicates that the retained substructure, owing to the incomplete recrystallization during solution treating, provides heterogeneous nucleation sites for the precipitation during subsequent ageing. The granular precipitates in the T6-tempered product have a size range between 0.05 and 0.2 μm . In the electron microscope, these precipitates can easily be distinguished from the Al-Fe-Si intermetallic particles fragmented from the needles during extrusion, because the latter are relatively larger. X-ray EDS shows that the precipitates have several compositions: ternary Al-Cu-Fe and quaternary Al-Si-Cu-Fe and Al-Si-Mg-Fe. However, no binary Al-Cu or Al-Mg phase is detected. Due to the interaction between the alloying elements involved in the present alloy, the precipitation process becomes much more complicated, and the ageing response of the present alloy may not be expected to follow the sequence of the formation of GP zone, transition phase and final phase, as typically occurs in Al-Cu alloys and Al-Cu-Mg alloys [31, 32]. Therefore, the understanding of the ageing process obtained from those alloys may not be applicable to the alloy presently being studied.

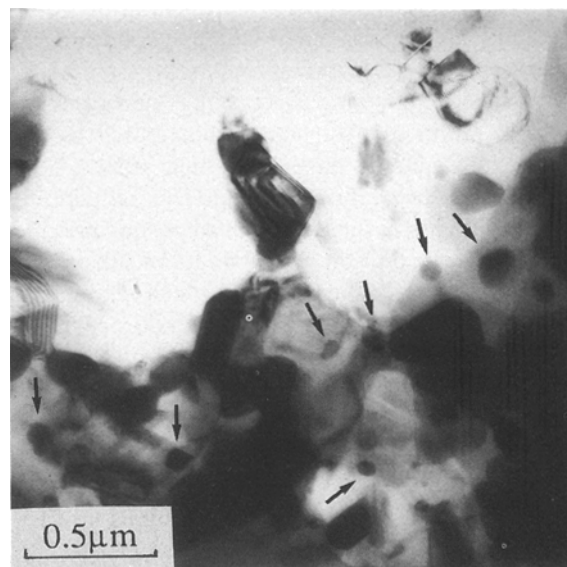


Figure 9 Electron micrograph of the aged Al-Si-Fe-Cu-Mg alloy, showing that precipitation occurs preferentially at the retained subgrain boundaries.

Clearly, the results from X-ray EDS are insufficient for identification of the precipitates, while their electron diffraction patterns are difficult to interpret owing to their complexity. Nevertheless, with the aid of knowledge of phase constitution, possible phases can be determined on the assumption that the heat-treated product has approached the equilibrium state after sequential processing. Considering 20 wt % Si, 3 wt % Cu and 1 wt % Mg involved in an aluminium alloy, such phases as $\text{Cu}_2\text{Mg}_9\text{Si}_5\text{Al}_4$, CuMgAl_2 and Mg_2Si should be formed, and these phases were indeed detected in the base alloy [18, 33]. However, in the present alloy with iron addition, the amount of these phases is too low to be detected with selected spot analysis. Most of the precipitates are found to contain iron and copper or magnesium. It confirms that, in the presence of 5% iron, copper and magnesium are mostly tied to form iron-bearing precipitates:

Cu_2FeAl_7 , CuFeAl_6 , and $\text{FeMg}_3\text{Si}_6\text{Al}_8$ [34]. In view of the chemical compositions, these phases correspond well with those shown in the spectra from X-ray EDS in the present work. It is thus clear that, due to the involvement of iron, a considerable amount of copper and magnesium is consumed in the iron-bearing precipitates. Apparently, the precipitation process of these phases is different from that in the alloys to which the T6 temper is applied as a standard scheme of heat treatment. Therefore, further study is desirable on the characterization and optimization of ageing through electron microscopic observation, in combination with differential scanning calorimetry analysis [31].

3.4. The effect of iron addition on tensile properties

In Figs 10 and 11, comparisons are presented of the variation of ultimate tensile strength with testing temperature between the present alloy and the base alloy, in the as-extruded and as-T6 tempered states, respectively. It can be seen that the 5% iron addition leads to a substantial improvement at all the temperatures and in both of the states. This apparently reflects the additional strengthening effects of fine particle dispersion and retained substructure contributed by iron-bearing intermetallic particles, which serve as extra obstacles to dislocation gliding. The reduction in strength with increasing temperature is similar in these two alloys. The addition of iron does not substantially alter the ductility of the material, which remains very limited. At 200 °C or below, fracture takes place on a transverse plane, before which there is almost no observable plastic deformation. It is important to mention that the data of tensile tests obtained from the T6-tempered material are much less erratic, and elongation values are somewhat enhanced, implying the occurrence of structural homogenization during

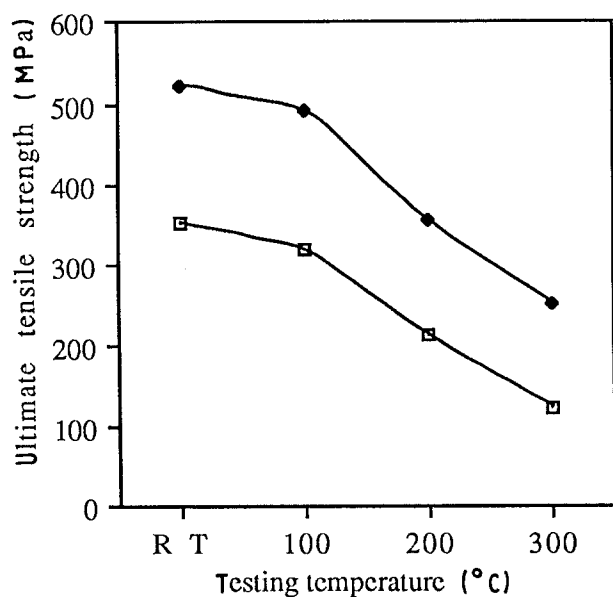


Figure 10 Variation of ultimate tensile strength of the alloys in the as-extruded state with testing temperature. \blacklozenge Al-20Si-5Fe-3Cu-1Mg extruded at 375 °C; \square Al-20Si-3Cu-1Mg extruded at 350 °C.

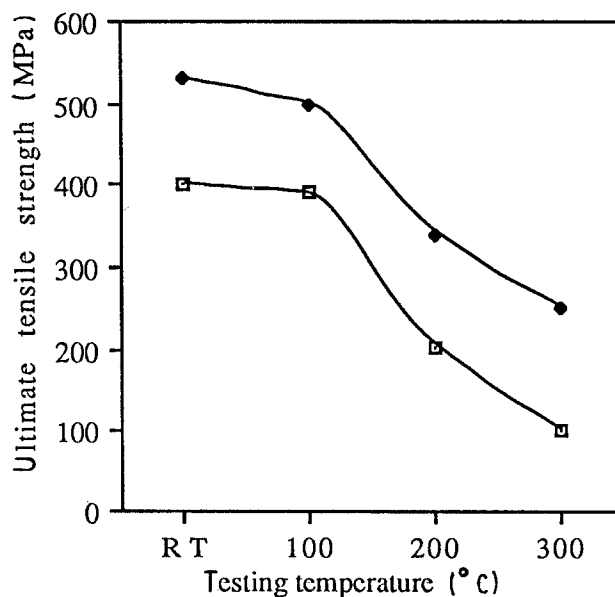


Figure 11 Variation of ultimate tensile strength of the alloys in the as-T6 tempered state with testing temperature. \blacklozenge Al-20Si-5Fe-3Cu-1Mg extruded at 375 °C and T6 tempered; \square Al-20Si-3Cu-1Mg extruded at 375 °C and T6 tempered.

the heat treatment. A comparison between the material before and after the T6 temper shows that, for the present iron-modified alloy, no improvement is obtained in strength at room temperature as a result of the heat treatment. This is in contrast to the base alloy, which shows an increase of about 50 MPa in strength. The reason for this may be that in the present alloy, iron ties a considerable amount of copper and magnesium to constitute iron-bearing precipitates which have been formed before the heat treatment. The strengthening effect given by copper- and magnesium-bearing precipitates, which is intended to be obtained through the T6 temper, becomes unmeasurable. At high temperatures the strength of the present alloy in both states stays at a same level, unlike that of the base alloy which exhibits a reduced strength at high temperatures after the T6 temper. The difference may be attributed to the fact that, in the present alloy, the strengthening due to additional iron-containing intermetallic particles, fine silicon particles and retained substructure overshadows the negative effect on high-temperature strengths given by the resolution of a very small volume fraction of copper- and magnesium-bearing precipitates. The reduction in strength properties owing to these unstable precipitates at temperatures above 200 °C was previously observed by the present authors [35], and has recently been confirmed in an Al-Fe-Zr-Cu-Mg alloy by Iwao *et al.* [36] who explain this reduction in terms of the influences of copper- and magnesium-bearing precipitates on work hardening rate, recovery rate and necking behaviour of the material. Clearly, in the present, highly alloyed aluminium, several strengthening mechanisms can be operative simultaneously. Of these, the dispersion strengthening given by the high volume fractions of silicon and Al-Fe-Si intermetallic particles undoubtedly plays a major role in determining the material strength, while in comparison the

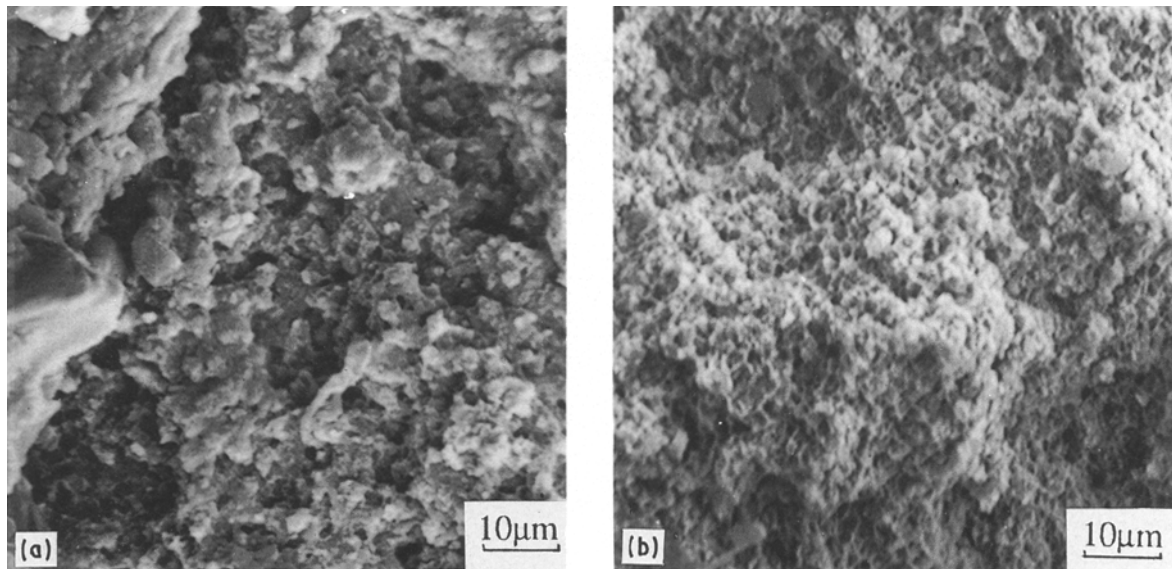


Figure 12 Scanning electron micrographs showing (a) fracture origin of the specimen tested at room temperature, and (b) uniform voids in the fracture surface of the specimen tested at 300 °C.

copper- and magnesium-bearing precipitates may not yield a substantial strengthening effect. It thus appears that the main merit of the T6 temper heat treatment applied is the structural homogenization, rather than further strengthening. The suggestion can therefore be made either to optimize the ageing effect so as to take the best advantage of material capability, or to simplify the alloy by removing the age-hardening elements, copper and magnesium, to alter the material to be non-heat-treatable. The latter could be more feasible in view of the dispersion strengthening as a major mechanism in the alloy desired to be used at elevated temperatures.

Figs 10 and 11 also reflect the thermal stability of the alloy. The microstructural observation of the material which has been exposed at testing temperatures up to 300 °C for 100 h does not reveal any noticeable changes. It means that the mechanical response of the alloy in service is only dependent upon the structure produced during processing. The dispersion of the thermally stable intermetallic particles, in combination with their inhibition both to the coarsening of silicon particles and to the growth of grains occurring during the heat treatment, is considered to be the key to the enhanced hot strength of the alloy. The present results clearly highlight the importance of creating and preserving a fine dispersion of particles to the material performance. At 300 °C, a tensile strength value of above 200 MPa is obtainable, which is markedly increased by about 100 % as compared with that of the base alloy. This level of strength, although not completely satisfactory, is adequate for the specific applications of the alloy, mainly in automobile engines. It is worth pointing out that the high-temperature strength of the present alloy may not compare favourably with that of rapidly solidified Al-Fe or Al-Cr alloys, but unique properties of the present alloy such as good wear resistance and a low thermal expansion coefficient [37–38] are not achievable in the other alloys.

The morphology of fracture surfaces examined by SEM (Fig. 12) indicates that void initiation at the interfaces of the dispersed phases and matrix, followed by coalescence, is the main failure mechanism. This is most evident at the testing temperature of 300 °C where a considerable plastic deformation allows the extended growth of voids, as shown in Fig. 12b. As the size range of the iron-bearing intermetallic particles is generally smaller than that of silicon particles, the void nuclei are considered to be preferentially formed at the interfaces between the silicon particles and matrix, where the stress concentration is more severe. This consideration is consistent with the fracture surface observation that the size of voids is associated with the silicon particle spacing which is very uniform, but not with that of the intermetallic particles. No apparent debonding between the original powder particles is found, which implies that sufficient interparticle bonding is produced during extrusion. However, at the temperature of 200 °C or below, fracture is observed to originate at the specimen surface where localized, typical brittle fracture features are shown, and thus fracture initiation promoted by the local imperfect bonding at the original powder particle boundaries cannot be precluded. The general fracture characteristics of the present alloy with a high volume of intermetallic particles are observed to be similar to those of the base alloy. Therefore, the fracture mechanisms described for the base alloy [39] may be applicable to the present alloy.

4. Conclusions

Complete recrystallization during the solution treatment at 470 °C for 1.5 h subsequent to extrusion is strongly inhibited by the iron-bearing intermetallic particles in the present alloy. Being inhomogeneously distributed, they perform a dual function of blocking the growth of recrystallized grains from particle-depleted areas, and of suppressing the recrystallization

nucleation and pinning subgrain boundary migration in the particle-rich areas. This results in a partially recrystallized duplex structure in the final product.

Coarsening of silicon particles during solution treating is lessened in the present alloy, which may be explained in terms of the blocking in the diffusion paths of silicon atoms by a high volume fraction of intermetallic particles. The exposure to the high temperature during solution treating does not give rise to any noticeable growth of the intermetallic particles.

Precipitation during ageing occurs preferentially at the retained subgrain boundaries. Iron ties a large amount of copper and magnesium to form ternary and quaternary phases. Thus, the conventional understanding of the precipitation process occurring in Al-Cu and Al-Mg alloys cannot be applied to the present alloy, and further research on the ageing characteristics of the alloy is needed.

From a practical point of view, we suggest the removal from the alloy of the age-hardening elements copper and magnesium, because their precipitates do not make a substantial contribution to the properties at the elevated temperatures at which the alloy will be used.

The addition of iron to the Al-Si-Cu-Mg alloy produces an important improvement in the strength of the alloy at room and elevated temperatures, which makes the alloy satisfactory to be used as a piston material in automotive engines.

Acknowledgements

The authors express their appreciation to the Showa Denko, K. K., Japan, for the provision of atomized powder used in this work. Financial support from the Program for Innovative Research (IOP) in the Netherlands (project 89-003, COST503) is gratefully acknowledged.

References

1. H. FREDRIKSSON, M. HILLERT and N. LANGE, *J. Inst. Metals* **101** (1973) 285.
2. WEIXING WANG and J. E. GRUZLESKI, *Mater. Sci. Technol.* **5** (1989) 471.
3. F. YILMAZ and R. ELLIOTT, *J. Mater. Sci.* **24** (1989) 2065.
4. J. KANEKO, M. SUGAMATA and K. AOKI, *Trans. Jpn Inst. Metals* **20** (1979) 733.
5. K. ICHIKAWA and S. ISHIZUKA, *ibid.* **28** (1987) 434.
6. K. MIWA, T. KAKAMU and T. OHASHI, *ibid.* **26** (1985) 549.
7. H. MATYJA, K. C. RUSSELL, B. C. GIESSEN and N. J. GRANT, *Metall. Trans.* **6A** (1975) 2249.
8. I. YAMAUCHI, I. OHNAKA, S. KAWAMOTO and T. FUKUSAKO, *Trans. Jpn Inst. Metals* **27** (1986) 187.
9. H. M. SKELLY and C. F. DIXON, *Int. J. Powder Metall.* **7** (1971) 47.
10. J. DUSZCZYK, J. L. ESTRADA, B. M. KOREVAAR, T. L. J. DE HAAN, D. BIALO, A. LEATHAM and A. OGILVY, in "Modern Developments in Powder Metallurgy", Vol. 19 (MPIF, New Jersey, 1988) p. 441.
11. M. VAN ROOYEN, P. F. COLIJN, TH. H. DE KEIJSER and E. J. MITTEMEIJER, *J. Mater. Sci.* **21** (1986) 2373.
12. M. VAN ROOYEN, N. M. VAN DER PERS, TH. H. DE KEIJSER and E. J. MITTEMEIJER, *Mater. Sci. Engng* **96** (1987) 17.
13. H. M. SKELLY and C. F. DIXON, *Powder Metall.* **10** (1976) 232.
14. N. AMANO, Y. ODANI, Y. TAKEDA and K. AKECHI, *Metal Powder Rep.* **44** (1989) 186.
15. T. HIRANO, F. OHMI, S. HORIE, F. KIYOTO and T. FUJITA, in Proceedings of an International Conference on Rapidly Solidified Materials, San Diego, California, February 1986, edited by P. W. Lee and R. S. Carbonara (ASM, Metals Park, Ohio, 1986) p. 327.
16. K. AKECHI, Y. ODANI and N. KUROIISHI, *Sumitomo Elec. Tech. Rev.* **24** (1985) 191.
17. J. ZHOU, J. DUSZCZYK and B. M. KOREVAAR, *J. Mater. Sci.* **23** (1990) 824-834.
18. J. ZHOU and J. DUSZCZYK, in Proceedings of the First European Conference on Advanced Materials and Processes, Aachen, West Germany, November 1989 edited by H. E. Exner and V. Schumacher, Vol. 1 (DGM Informations gesellschaft-Verlag, Oberursel, (1990) p. 241.
19. H. J. MCQUEEN, E. H. CHIA and E. A. STARKE, *J. Metals* **38** (1986) 19.
20. P. N. KALU and F. J. HUMPHREYS, in Proceedings of the 7th Risø International Symposium on Metallurgy and Materials Science, Risø, Denmark, September 1986, edited by N. Hansen, D. J. Jensen, T. Leffers and B. Ralph, (Risø National Laboratory, Roskilde, Denmark, 1986) p. 385.
21. P. FURRER and G. HAUSCH, *Metal Sci.* **13** (1979) 155.
22. V. STEFANIAY, A. GRIGER and T. TURMEZEY, *J. Mater. Sci.* **22** (1987) 539.
23. T. HIRANO and T. FUJITA, *Trans. Jpn Inst. Light Metals* **37** (1987) 670.
24. F. J. HUMPHREYS, *Acta Metall.* **25** (1977) 1323.
25. B. BAY and N. HANSEN, *Metall. Trans.* **10A** (1979) 279.
26. F. R. CASTRO-FERNANDEZ and C. M. SELLARS, *Mater. Sci. Technol.* **4** (1988) 621.
27. D. L. LLOYD, *Metal Sci.* **16** (1982) 304.
28. S. S. EZZ, A. LAWLEY and M. J. KOCZAK, in Proceedings of a Symposium on Dispersion Strengthening Aluminum Alloys (1988 TMS Annual Meeting), Phoenix, Arizona, January 1988, edited by Y-W Kim and W. M. Griffith (TMS, Warrendale, Pennsylvania, 1988) p. 243.
29. E. A. STARKE, Jr. and J. A. WERT, in Proceedings of a Symposium on Aluminum Powder Metallurgy (1985 TMS-AIME Meeting) Toronto, Canada, October 1985, edited by G. J. Hildeman and M. J. Koczak (AIME, Warrendale, Pennsylvania, 1985) p. 3.
30. U. V. DESHMUKH, S. KUMAR, M. J. KOCZAK and C. ROAMNOWSKI, *ibid.* p. 79.
31. L. KATGERNAMN and B. VAN DEN BRANDT, *ibid.* p. 65.
32. C. M. FRIEND and S. D. LUXTON, *J. Mater. Sci.* **23** (1988) 3173.
33. J. DUSZCZYK, J. L. ESTRADA, B. M. KOREVAAR, Z. FANG, T. L. J. DE HAAN and P. F. COLIJN, "Processing of P/M Rapidly Solidified Al-Si-X Aluminium Alloys for Wear and High-Temperature Resistance Applications", Technical Report for Showa Denko K. K. Japan (Delft University of Technology, The Netherlands, October 1987).
34. L. F. MONLDOFO, "Aluminium Alloys, Structure and Properties" (Butterworth, London, 1976) p. 759.
35. J. ZHOU and J. DUSZCZYK, *J. Mater. Sci.* in press.
36. O. IWAO, J. SHIMZU and P. A. SODERGRÉN, in Proceedings of Light Metals 1989, Las Vegas, Nevada, February 1989 (TMS-AIME, Warrendale, Pennsylvania, 1989) p. 725.
37. D. BIALO, J. DUSZCZYK and T. L. J. DE HAAN, "Mechanical and Microstructural Aspects of Fretting Wear of P/M Aluminium Alloys and Composites", Internal Report (Delft University of Technology, The Netherlands, October 1989).
38. D. BIALO, J. DUSZCZYK, A. W. J. DE GEE, G. J. J. VAN HEIJNINGEN and B. M. KOREVAAR, *Wear* (in press).
39. J. ZHOU and J. DUSZCZYK, *J. Mater. Sci.* **25** (1989) 4541-4548.

Received 19 April
and accepted 16 May 1990